Electronic transport in films of colloidal CdSe nanocrystals

Nicole Y. Morgan[1], C.A. Leatherdale[2], M. Drndic[1], Mirna Vitasovic[2], Marc A. Kastner[1], Moungi Bawendi[2],
[1]*Dept. of Physics,* [2]*Dept. of Chemistry, M.I.T., 77 Massachusetts Ave., Cambridge MA 02139*
(February 1, 2008)

We present results for electronic transport measurements on large three-dimensional arrays of CdSe nanocrystals. In response to a step in the applied voltage, we observe a power-law decay of the current over five orders of magnitude in time. Furthermore, we observe no steady-state dark current for fields up to 10^6 V/cm and times as long as 2×10^4 seconds. Although the power-law form of the decay is quite general, there are quantitative variations with temperature, applied field, sample history, and the material parameters of the array. Despite evidence that the charge injected into the film during the measurement causes the decay of current, we find field-scaling of the current at all times. The observation of extremely long-lived current transients suggests the importance of long-range Coulomb interactions between charges on different nanocrystals.

81.07.Ta, 77.22.Jp

Introduction

The techniques of colloidal chemistry make it possible to create vast numbers of nearly identical semiconductor nanocrystals[1,2]. Measurements of the tunneling of electrons onto individual nanocrystals have demonstrated that the latter behave qualitatively like lithographically defined quantum dots[3]; such structures are best described as artificial atoms because their energy and charge are quantized[4,5]. Although it is difficult to construct large arrays of lithographically patterned artificial atoms, colloidal nanocrystals assemble themselves into such arrays quite naturally, creating an entirely new class of solids composed of artificial atoms. Furthermore, by adjusting the chemical process, it is possible to tune physically relevant parameters, such as site energies and nearest-neighbor coupling. We report here studies of electron transport in such a Colloidal Artificial Solid (CAS).

Our CAS is composed of CdSe nanocrystals ~ 5 nm in diameter, each capped with organic molecules ~ 1 nm long. Because of the small size of the nanocrystals the Coulomb interaction between two electrons on the same nanocrystal or adjacent nanocrystals is ~ 0.1 eV[6], larger than k_BT at room temperature. It is likely, therefore, that the Coulomb energy is larger than the other important energies in the problem, in particular the bandwidth resulting from inter-nanocrystal tunneling or disorder. Thus, these CASs provide an interesting new system in which the motion of electrons is expected to be highly correlated[7].

Although the optical properties of these nanocrystal systems have been studied extensively, as yet there has been little work on electronic transport in these arrays. In this work, we present measurements made on a lateral, gated device, shown in Fig. 1; this geometry has two primary advantages over the simpler sandwich structure used by Ginger and Greenham[8]. First, because the nanocrystal films are deposited last, there is no possibility of damaging the films during device fabrication. Second, the gate electrode provides the possibility of controlling the charge density in the CAS.

We find that films of CdSe CASs are extraordinarily resistive, with resistivity greater than $\sim 10^{14}$ ohms-cm at temperatures below 200 K. Although there is no detectable steady-state current, we observe current transients after the application of a voltage step; the current decays as a power law in time out to at least 10^4 s. When the film is located near a metal gate, we can directly observe the buildup of charge in the sample, which, at low temperatures, then remains in the CAS even after the voltage is removed. Although this suggests that the decay of the current is associated with the charging, the integral of the current transient is orders of magnitude larger than the charge stored. Thus, we conclude that the current arises from charge which moves completely through the film, but that the sample becomes more resistive with time as more charge is injected. We suggest that these effects are related to the strong Coulomb correlations between electron occupancy of the nanocrystals. In this paper, we present transport measurements on this system as a function of device geometry, applied field, sample length, and temperature, as well as some preliminary data on variations of the transients with the parameters of the chemical synthesis.

Experimental details

The synthesis of the CdSe nanocrystals and the deposition of the close-packed films has been described in detail previously[9,10]. By using the organo-metallic synthesis of Murray, *et al.* followed by three steps of size-selective precipitation, a size distribution with variance $\sigma = 5 - 8\%$ is typically obtained. For most of the measurements in this paper, the nanocrystals are covered with a monolayer of tri-octylphosphine oxide (TOPO), as a byproduct of the synthesis. These molecules serve to passivate the surface states of the nanocrystals, and also act as nearest-neighbor spacers when the nanocrys-

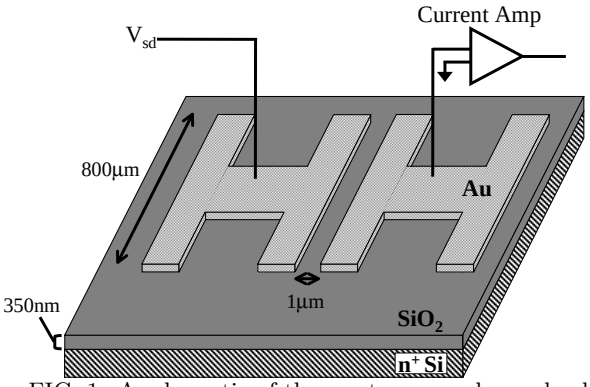

FIG. 1. A schematic of the most commonly used substrate and electrode structures. The base material is a standard commercial (100) silicon wafer, degenerately doped with arsenic. The 350 nm thick oxide is thermally grown, and the electrodes (200 Å Ti, 2000 Å Au) are patterned with a single optical lithography step and a lift-off technique. When the nanocrystal film is deposited, it covers the entire surface, including the electrodes. The associated measurement circuit is described in the text.

tal films are formed. For some samples, after the synthesis the capping molecules have been exchanged from TOPO to tri-butylphosphine oxide (TBPO), which gives a smaller nearest-neighbor separation; the procedure for the exchange has been described elsewhere[11]. For the work discussed here, the nanocrystals typically have a core diameter of approximately 4.5 nm; those capped with TOPO have a 1.1 nm nearest-neighbor separation, and those with TBPO have a 0.7 nm nearest-neighbor separation[10]. The films are formed by drop-casting a solution of nanocrystals in 9:1 hexane/octane, which is allowed to dry for a minimum of two hours in an inert atmosphere before exposure to vacuum. To a first approximation, the thickness of the films is controlled by the concentration of the solution; for the work reported here, the thickness of the films ranges between 20 and 180 layers ($100 - 900$ nm), as measured with a profilometer near the measurement electrodes. Direct imaging of the nanocrystal packing on the measurement substrates has proven difficult, but transmission electron microscope images of similarly prepared films suggest that the ordering within the CAS is polycrystalline, with the typical grain size approximately 10 nanocrystals across[12].

The primary type of device structure used for this work is shown in Figure 1. These structures have been produced in large quantities so that many films, some with different core sizes and different capping molecules, can be deposited on identical devices. The starting material is a (100) silicon wafer degenerately doped with arsenic (room temperature sheet resistance 1–5 mΩ), which is used as the back gate for the device. High-quality thermal oxides of 350–500 nm are grown on top of these substrates, and then 200 nm Ti-Au electrodes are patterned and deposited using optical lithography and a lift-off procedure. We have also made measurements on films deposited on 0.5 mm quartz wafers, for which the gold electrode pattern is identical, but for which the electrodes are only 110 nm thick. In both cases, although only one set of electrodes is depicted in Fig. 1, there are many more electrodes, some with different gap sizes, on each wafer. The full size of the substrate is typically 6×6 mm, and the size affects the spreading of the nanocrystal solution during film deposition. In addition, for some measurements we have used ring-shaped electrodes (not shown) with a similar gap size for a few experiments, for which the results are consistent.

The fabrication of the substrates is completed before the nanocrystals are deposited and then dried overnight in an inert atmosphere; afterwards, the nanocrystal film covers the entire substrate, including the electrodes. Depositing the nanocrystals as the final step in sample preparation is important. These films are not sufficiently robust to permit the use of standard wafer processing techniques after deposition. In particular, subsequent measurements have shown that even moderate heating, to 100 deg C in vacuum, can significantly affect the transport and optical properties of the films[12]. The electrode geometry and the measurements are chosen to give a well-defined active area for the device, as will be discussed below. For the most common samples, 4.5 nm core-diameter, TOPO-capped nanocrystals, and the electrode configuration of Fig. 1 there are approximately 200 dots in series and about 160,000 dots in parallel for one layer of dots. Room-temperature optical measurements of nanocrystal films co-deposited on glass slides are used to ensure sample quality.

The electrical measurements are made in an Oxford Variox cryostat, with the sample in vacuum, typically at liquid nitrogen temperature. The current is measured with a Keithley 427 current amplifier; depending on the voltage and time ranges of interest, one of several voltage sources, including a Yokogawa 7611, a HP 3245, and a Kepco BOP-500V, is used. In a typical measurement, a voltage step is applied at one of the electrodes, and the current is measured at the other electrode as a function of time, with the back gate grounded. Throughout this paper we will refer to the electrode at which the voltage step is applied as the source, and to the current measurement electrode as the drain, as indicated in Fig. 1. For the gated silicon substrates, this measurement is asymmetric in voltage when the gate is grounded; because the drain electrode is connected to the input of the current amplifier, which is a virtual ground, the field at the source is much larger than that at the drain. As a result, charge is only injected into the film from the source electrode for the gated substrates. Furthermore, although charge spreads into the film in all directions from the source, the measurement at the drain electrode is sensitive only to charge moving between the electrodes, as more distant charge will be screened by the gate[13]. Finally, this measurement is not directly sensitive to leakage currents between the source and the gate, and there is no field to generate leakage current between the drain electrode and

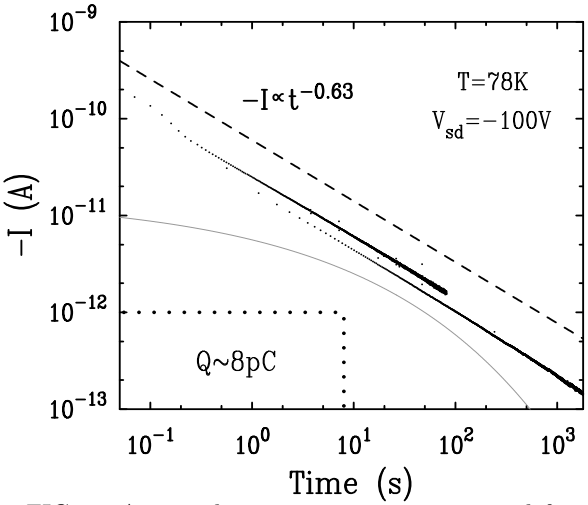

FIG. 2. A typical current transient, measured for a CAS with 45 Å core-diameter, TOPO-capped nanocrystals on a substrate with a 350 nm gate oxide, at 78K. With the gate grounded, the source voltage is stepped to −100 V, and the current at the drain electrode is measured as a function of time. Two measurements, with different circuit response times, are shown; the difference in the amplitudes of the two transients reflects sample history effects. The dashed line represents a power-law decay of the current, with an exponent of −0.63. The rectangle outlined by a dotted line in the lower left corner represents an upper bound for the amount of charge expected from capacitive charging of the quantum dot film in the gap between the measurement electrodes. The deviation from power-law behavior at short times varies with the series resistance and is therefore ascribed to charging of geometrical capacitances.

the gate.

Results

As mentioned above, the CAS films are highly resistive. For a film of 4.5 nm diameter CdSe nanocrystals we measure no steady-state current for applied fields of up to 10^6 V/cm, which corresponds to an average nearest-neighbor potential difference of 500 mV. With a current detection limit of 5 fA, and the device geometry used here, this gives a lower bound for the resistivity of of $\sim 10^{14}\Omega$-cm; no steady state current has been observed in any of the dozens of samples we have studied. However, the time dependence of the current in response to an applied source-voltage step is unusual. Figure 2 shows a plot of the typical current measured at the drain electrode as a function of time; unless otherwise noted, the gate is grounded in all of the transient measurements. At $t = 0$, the voltage at the source electrode has been stepped from zero to -100 V, after which the resulting current decays with a power-law form. In other measurements, the power-law decay of the current has been observed to persist overnight, to approximately 2×10^4 seconds. Together with the data are plotted two fits, displaced vertically for clarity. Above the data is a power law, $I = I_1 t^{-\alpha}$, with $\alpha = -0.63$, and below the data is a stretched exponential $I = I_0 \exp -(t/\tau)^{\beta}$, with the characteristic time τ set at 1 ms. Clearly, the data are better described by a power law form.[14]

For the various nanocrystal samples measured, the decay exponent, α, ranges from -0.1 to -1; the parameters upon which α depends are discussed below. Thus, the charge obtained from integrating the transient current diverges in time. By itself, this divergence suggests that the current is not just the displacement current that arises from the polarization or to the buildup of charge in the CAS. In fact, the value of the integrated current over a typical measurement time of 10^3 seconds is several orders of magnitude greater than the estimate for charge stored in the film. To illustrate this, in the lower left of Figure 2, we have drawn a dotted rectangle, which represents the amount of charge that would reside in the film, if the entire active area between source and drain were charged to the full potential of the applied voltage step, V_{sd} with respect to the gate electrode.[15] Here, this estimated charge is approximately 8 pC, whereas for the transient shown in Fig. 2, the integrated current exceeds this value by more than two orders of magnitude. Were this measurement not truncated the disparity would be greater still. We conclude that the current arises from charge which travels through the sample, and that the current decays because the film grows more resistive with time.

Nonetheless, we believe that the increase of the resistance over time is related to the buildup of charge in the CAS. The injection of charge into the film can be directly measured by applying voltage to the gate electrode while measuring the current at one of the top electrodes; for this type of measurement the source and drain are both held at ground potential and are therefore equivalent. As noted above, there are many other electrodes on the top of the oxide in contact with the CAS film, and these are all at the same potential as the source and drain. Although charge spreads into the film from all of these electrodes, typically the current is measured only at one of them; furthermore, this current arises only from the charging of the nanocrystal film.

The response of the sample to the gate voltage is shown in Figure 3, for three consecutive ten minute steps. In the first step, the gate voltage is stepped to +100 V, and negative charge flows slowly into the film from the top electrodes; after ten minutes the current is still nonzero. In addition to this slow charging, at short times there is also a contribution from the displacement current, which corresponds to the charging of the capacitance between the measuring electrode and the gate. In the second step, when the gate voltage is stepped back to zero, only this displacement current is observed. Any current that might indicate a discharge of the nanocrystal film is below the noise floor, which is approximately 0.01 pA for this measurement. After being held with $V_g = 0$ V for ten minutes, in the third step the sample is illuminated with

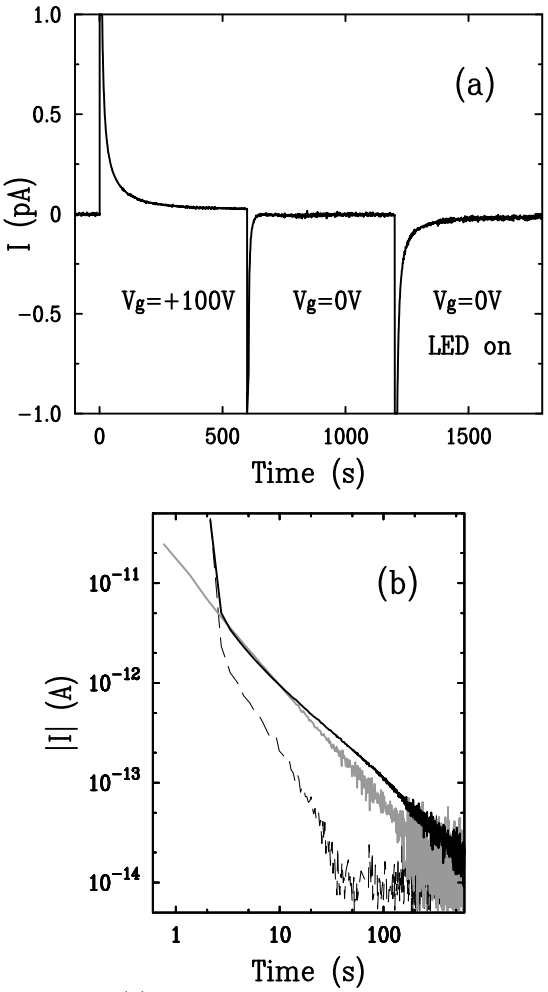

FIG. 3. (a)Current transients measured at one of the top electrodes for a series of ten-minute gate voltage steps at 78K. The measurement electrode is grounded through the current amplifier; all other top electrodes are directly grounded throughout. Integrating the current, including the fast capacitive component, gives 85 pC for the first step, in which V_g is stepped to +100V; −34 pC for the second step, in which V_g is stepped back to 0 V; and −46 pC for the third step, in which V_g is held at zero and the sample exposed to band-gap light. The 34 pC in the second step is consistent with estimates of the charge on the geometrical capacitance. (b) The absolute value of the same three current transients, plotted on a logarithmic scale. The first transient ($V_g \rightarrow 100$ V) is shown in black, and clearly shows a fast capacitive component at short times and an approximate power-law decay at long times. The second transient ($V_g \rightarrow 0$ V) is shown as a dashed line, and shows only the fast capacitive component, followed by a very small component attributed to polarization of the substrate. Transients measured for $V_g \rightarrow -100$ V are identical to this second transient, i.e., they show no evidence of charge injection. The third transient (LED on) is shown in gray, and decays as a power-law with an exponent of −1.2. Note the absence of the capacitive component, as well as the similarity between the time dependence of the discharging and that of the charging in the first transient.

band gap light from a light-emitting diode (LED) near the sample in the cryostat. The wavelength of the LED has been chosen to match the absorption peak of the CAS. This illumination causes the charge to be released from the film. The integral of the total current for each time period is indicated in the figure caption. The total charge integrated over the entire process is very small, which indicates that most of the charge which was injected in the +100 V step is removed by exposure to the LED.[16]

Figure 3b shows the same data for the charging and discharging of the CAS on a logarithmic scale. Interestingly, the time decay of the discharge under illumination is very similar to that of the charging; in both, the current has an approximate power law form, although the decay here is steeper than for the source-drain measurements. Since the decay of the current follows approximately t^{-1}, the charge spreads only logarithmically in time. From the perimeter of the H-shaped electrodes, approximately 4.4 mm, and the 350 nm thickness of the gate oxide, we calculate the surface charge density at which the nanocrystal film is charged to 100 V. Using this calculated density and the value of the stored charge, 46 pC, measured from the light-induced discharge, we estimate that the injected charge has spread out roughly 1.1μm from the electrode during the ten-minute charging step.

There is also a clear difference between the current during the first step, with $V_g = +100$ V, and that in the second step, for which the voltage is stepped back to zero. In the latter transient, the expected capacitive transient is seen at short times (≤ 3 s). At longer times there is a low-level current which decays relatively rapidly. This background transient, unlike the charging of the film, is linear in voltage; we believe that it results from polarization of the oxide. Like the measurements of Fig. 2, These gate charging measurements exhibit a strong asymmetry with the sign of the applied voltage. When the gate voltage is stepped to −100 V rather than to +100 V, only the polarization current is observed; there is no evidence for the injection of positive charge into the CAS. In addition, if negative charge has previously been injected by applying a positive gate voltage, application of a negative gate voltage removes little of this charge. At $T = 78$ K, the stored charge can only be removed from the system on time scales on the order of minutes by illumination with band-gap light. Warming the sample to room temperature also releases the stored charge and returns the CAS to its initial state, although the process is considerably more time-consuming.

The release of the stored charge when the sample is illuminated with band-gap light suggests that the injected charge resides predominantly on the nanocrystals, rather than within the organic capping molecules or at defects on the (substrate) oxide surface. This is more strongly supported by measurements of changes in the absorption spectra with applied voltage in sandwich structures by Woo *et al.*[17]. For the same electrode material and applied fields similar to those used in this work, Woo *et al.*

also observe a quenching of the nanocrystal photolumi nescence consistent with charging of the nanocrystals.

From the above data we can already eliminate two sim ple explanations. First, we are measuring properties c the CAS, rather than leakage through the substrate o conduction through the organic which fills the interstice of the nanocrystal film. Similar measurements on a bar substrate show no charge injection or power-law curren transients. Also, in several instances we have made elec trical measurements on films for which optical spectra taken later, showed the nanocrystals to be somewha oxidized; these oxidized samples, while exhibiting ver weak photocurrent, showed no measurable current injec tion in the dark, although the organic molecules were th same as in the other samples. Finally, as discussed tc wards the end of this section, we see variations in th current transients with changes in the parameters of th CAS; in future work we hope to look at these variation in more detail. However, we note that although the in jected charge appears to reside on the nanocrystals, a this time we are unable to distinguish between charg which resides in the nanocrystal core and charge whic resides in a surface state of the nanocrystal.

Second, the samples appear to be chemically stable un- der these measurement conditions; several samples have been measured for over three weeks, with no evidence for degradation. Although there are long-lived history effects associated with the charging of the samples, it is possible, either by briefly warming to room temperature or illuminating with band gap light, to remove the stored charge. As long as the sample is kept in vacuum and cold, the measurements for a particular sample are reasonably reproducible. For the remainder of the results section we examine the details of this transient behavior as a func- tion of sample length, gate oxide thickness, temperature, and array parameters.

Just as the film accumulates charge when voltage is applied to the gate, the film must accumulate charge at the oxide interface, possibly across the length of the sam- ple, when voltage is applied to the source with the gate grounded. Immediately after the application of a volt- age step at the source, before any charge is injected into the film, the field is not uniform across a gated sample. Rather, for a particular applied voltage, the thinner the gate oxide, the stronger the field is near the source con- tact. To determine the effect of the gate we have made measurements on gated samples with several oxide thick- nesses, as well as on quartz substrates, for which the gate is 0.5 mm distant and therefore does not affect the fields across the 1 and 2 μm gaps. However, we note that even for the silicon substrates with a 350 nm gate oxide, the distance to the gate is a substantial fraction of the elec- trode separation; relatively thick gate oxides were neces- sary to permit the application of the large fields necessary to pass charge through the samples.

Because there is no gate to influence the field across the electrode spacing for the quartz substrates, it is straight- forward to study the dependence of the power-law tran-

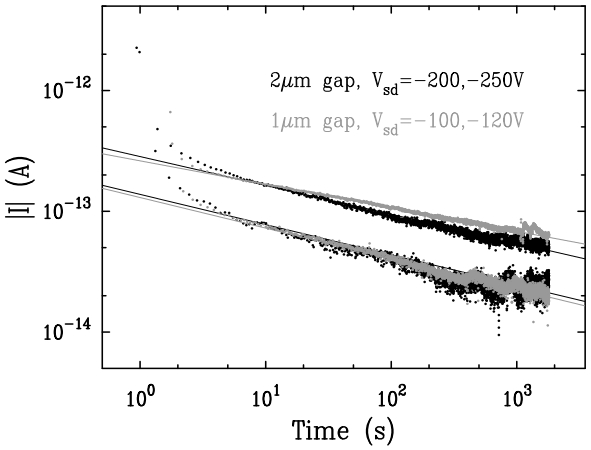

FIG. 4. Two sets of transients for a single film of 49 Å core-diameter, TOPO-capped nanocrystals, measured on a quartz substrate with two different electrode spacings but similar applied fields. For the 2 μm sample length, the transients, plotted in black, are for steps of $V_{sd} = -200$ V and $V_{sd} = -250$ V; for the 1 μm sample length, the transients are plotted in gray, and correspond to steps of $V_{sd} = -100$ V and $V_{sd} = -120$ V. The solid lines are the associated power-law fits, the parameters of which are plotted in Fig. 5. $T = 79$ K.

sients on sample length. Two pairs of transients are plot- ted in Figure 4 for a CAS on quartz; transients measured on a sample 2 μm long, with $V_{sd} = -200$ and -250 V, are shown in black, and transients measured for a 1 μm long sample, with $V_{sd} = -100$ and -120 V are shown in gray points. The solid lines are the corresponding fits to a power-law form, $I(t) = I_1 t^{\alpha}$. There is reasonably good agreement between the transients measured at the same fields for the two different sample lengths.

The parameters of these power law fits have been plot- ted in Figure 5. The data for the 2 μm sample length are shown in open triangles, and the data for the 1 μm sample, with the voltage rescaled by a factor of two, are shown in open squares. The close agreement between the rescaled data for the 1 μm sample and that for the 2 μm sample provide further evidence that the current transients depend only on the applied field.

The results on quartz are generally consistent with the measurements on the gated silicon substrates, in that we still observe power-law current transients, and again see no evidence of steady-state current. The major quanti- tative difference is that the values for α are smaller than those observed for the gated substrates. Power-law fits to two sets of current transients measured on a quartz substrate yield the data in Figure 5, which shows the de- cay exponent, α, as well as the logarithm of the current at 10 s, both as functions of the source-drain voltage. Note that one can apply much larger voltages than for the gated devices, because the insulator is much thicker. Furthermore, because the distance to the gate is much greater than the distance between the electrodes, one ex- pects approximate symmetry for positive and negative voltages for the quartz substrates, whereas we observe

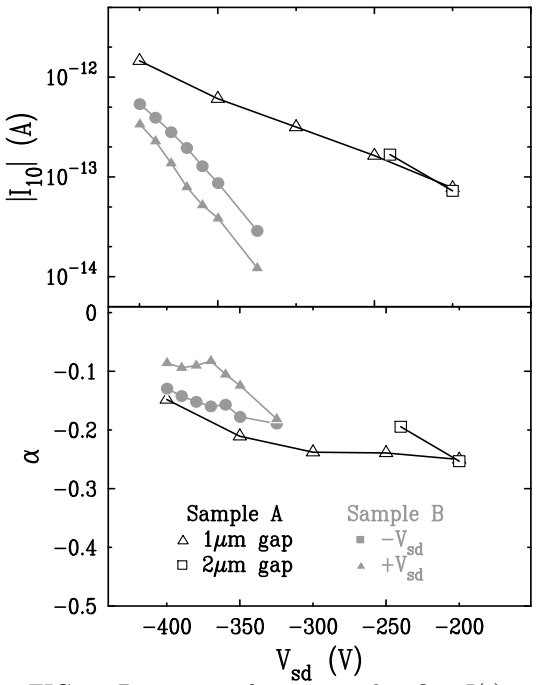

FIG. 5. Parameters from power-law fits, $I(t) = I_{10}(t/10s)^{\alpha}$ to current transients measured on TOPO-capped CdSe nanocrystals deposited on a quartz substrate, plotted as a function of applied voltage. Top panel: the amplitude of the current transients at ten seconds. The approximately exponential dependence of the transients on applied voltage is typical of measurements made on quartz substrates. Lower panel: the decay exponent of the transients. The fluctuations in the decay exponent above $|V_{sd}| = 350$ V within a single data set are within the fitting error. Note that while the exponents are quite consistent, the magnitude of the current and its voltage dependence are not reproducible. The points corresponding to the measurements of Figure 4 are shown in open symbols; the triangles correspond to data for the 2 μm sample length, and the squares to data for the 1 μm sample length, after the voltage has been rescaled by a factor of two. The agreement between the 2 μm data and the scaled 1 μm data reflect the field-scaling discussed in the text. Data for another sample, of the same diameter (49 Å), are shown in filled symbols, for both signs of the voltage. Filled circles correspond to data for $-V_{sd}$, and filled triangles to data for $+V_{sd}$. The discrepancy between the two signs of voltage most likely arises from sample history effects.

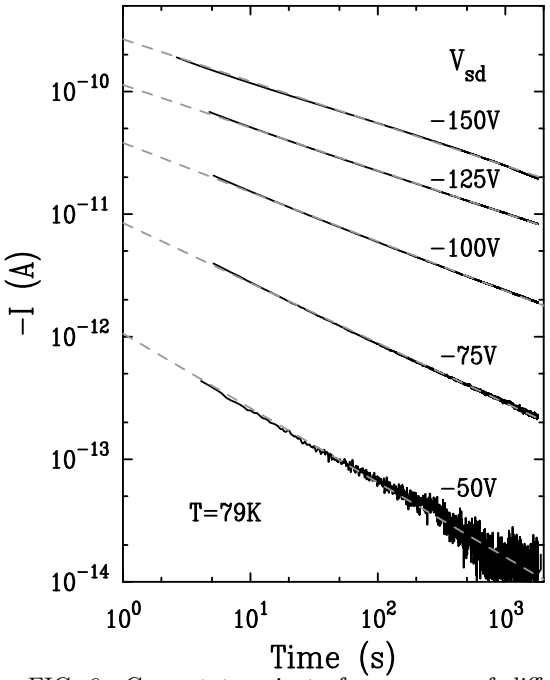

FIG. 6. Current transients for a range of different voltage steps, for a TOPO-capped, 45 Å core-diameter sample measured on a 1 μm gap, on a substrate with a 350 nm oxide. The sample had been cooled with $V_g = -150$ V several hours earlier; measurements on samples cooled with $V_g = 0$ V show similar behavior, but smaller amplitudes for the current transients, as discussed in connection with Fig. 9. Steps are made in order of increasingly negative voltage, with a half-hour $V_{sd} = 0$V step in between, during which the sample is illuminated for twenty minutes. Transients are not observable for positive V_{sd}. $T = 79$K and $V_g = 0$V throughout. Dashed lines are power-law fits to the data; the parameters from these fits are plotted in Fig. 7.

current transients only for negative source voltages for the Si substrates. The small asymmetry seen in Fig. 5 for measurements on a single sample are likely the result of sample history; we believe that some charge is stored in the CAS even when the gate is remote. The discrepancy between the two different samples is somewhat more difficult to understand, but may arise from differences in sample preparation or film thickness.

As seen in Figure 5, the current at fixed time increases exponentially with the applied voltage for the CAS on a quartz substrate. For the gated samples, however, the voltage dependence is more complex. Figure 6 shows transients for a range of voltages, measured for a sample on a 350 nm oxide. For similar voltages, the currents at 10 s are considerably larger for the gated substrates, allowing us to measure transients at lower voltages; this is probably the result of higher fields in the sample near the source electrodedue to the presence of the gate. In Fig. 7 the parameters obtained from fits of a power-law decay to these transients are plotted, together with a set of points corresponding to a nominally identical sample with a similar history, all in filled black symbols. There is

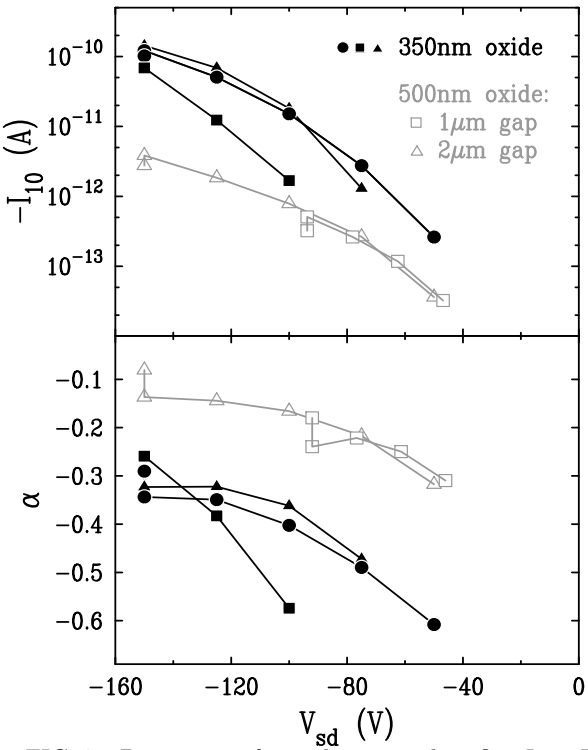

FIG. 7. Parameters from the power-law fits $I = I_1 t^\alpha$ to current transients measured for samples on gated substrates. Top panel: the amplitude of the transients at ten seconds. Lower panel: the decay exponent of the transients. Data for 1 μm long samples on substrates with a 350 nm gate oxide are shown in black; the filled circles correspond to the dashed lines in Fig. 6, and the triangles come from measurements taken on a different but nominally identical sample. The filled squares correspond to measurements on the first sample, immediately after cooling with $V_g = 0$V. Data for a sample of 45 Å diameter nanocrystals measured on a substrate with a 500 nm oxide substrate are shown in gray, for two different sample lengths. The open triangles correspond to the 1 μm sample, and the open squares are data for the 2 μm long sample, after dividing the voltage by a factor of 1.6. Transients are only observed for negative V_{sd} on the gated substrates.

remarkably good agreement between the two sets of data. On the same axes are also plotted another set of points, which correspond to a set of transients measured for a sample on a substrate with a 500 nm oxide. For both types of gated substrate, the decay exponents become smaller with more negative V_{sd}, and the amplitude of the current at 10 s, as well as the exponent α, appear to saturate as the size of the voltage step is increased.

Although the current transients scale with field on the quartz substrates, the scaling with applied voltage is different for samples measured on gated substrates[18]. For a 500 nm thick oxide, although we can find a voltage such that the transient on the 2 micron gap is the same as that on the 1 micron gap, the voltages differ by a factor of 1.6 instead of 2. Interestingly, this single rescaling factor persists over the entire voltage range for which the transients are measurable. This is illustrated in Fig. 7, where the data for the 500 nm oxide substrates consist of data for a 1μm sample, shown in open triangles, as well as rescaled data for a 2 μm sample, shown in open squares. The scaling factor appears to be smaller still for the 350 nm oxide. Thus it appears that the transients on quartz substrates depend only on the field, whereas for the silicon substrates, as the gate oxide thickness is reduced, the transients become less dependent on the electrode spacing, perhaps approaching a dependence only on the source voltage.

The temperature dependence of the current transients is shown in Figure 8, for measurements of a 1 μm long sample on a substrate with a 350 nm gate oxide; these parameters are obtained from three-parameter power-law fits to the transients, $I(t) = I_1 t^\alpha + I_{leakage}$. In the top panel, the current at ten seconds is plotted for three different values of V_{sd}. Also shown is the steady-state leakage current, which is identical to that measured on an equivalent device structure with no CAS film. This leakage current is linear in voltage, and is well described by an activated form, $I = I_0 \exp(-E_A/k_B T)$, with an activation energy $E_A = 370$ meV. Clearly, the leakage current interferes with the measurements of the transients at temperatures above ~ 220 K. The decay exponent of the current transients is plotted in the lower panel. Although Fig. 8 shows only data from 77K to room temperature, a separate set of measurements from 6K to 77K shows no substantial variation with temperature over that range. Above 77K, there is little variation in either of the parameters until approximately 150K, above which the amplitude of the current transients increases and the power law becomes steeper. The decrease in the amplitude of the transients above 220 K, and the associated sharp drop in the decay exponent, is most likely an artifact associated with the leakage current.

In order to further explore the relationship between the buildup of charge in the CAS and the current transients, we have measured transients after cooling the samples with an applied electric field. At room temperature, a voltage V_{fc} is applied to the gate, and the sample is then cooled to 77 K. Once the sample is cold, the gate

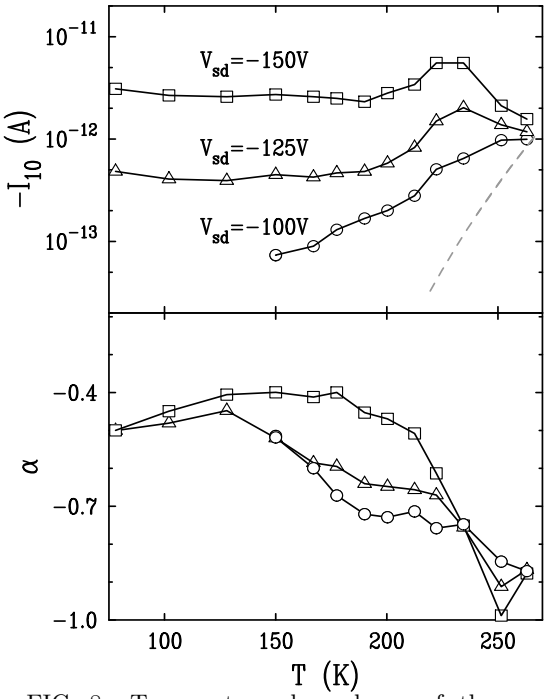

FIG. 8. Temperature dependence of the current transients measured on the same sample as in Fig. 6, taken in order of increasing temperature. The two parameters are obtained from three-parameter fits to the transients, $I(t) = I_{10}(t/10s)^{\alpha} + I_{leakage}$, where $I_{leakage} = 0$ for $T < 200$ K. Top panel: the amplitude of the current transients at ten seconds. The dashed line indicates the value of I_{ss} for $V_{sd} = -100$ V, which is identical to that measured on a bare substrate, and so is attributed to oxide leakage. Lower panel: the decay exponent of the transients, for the same values of V_{sd}. Note that the transients for $V_{sd} = -100$ V are too small to fit below 150 K.

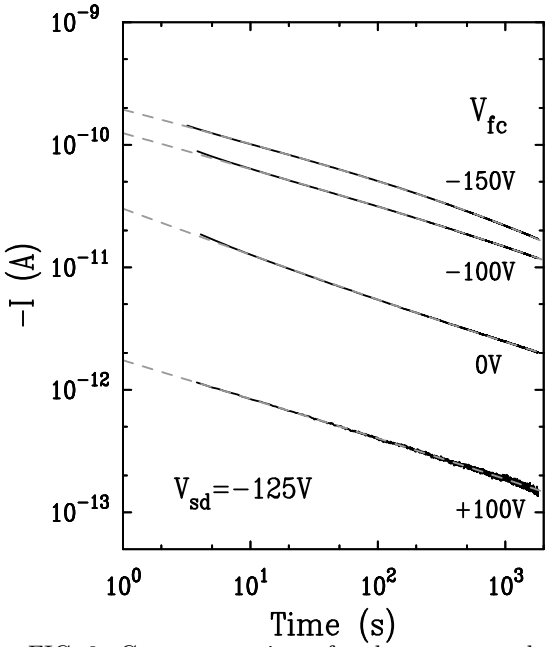

FIG. 9. Current transients for the same sample as in Fig. 6, after cooling with different gate voltages, shown with power-law fits (dashed lines). Before each transient, the sample has been prepared by cooling from approximately 290K to 78K with V_{fc} (labelled on the right) applied to the gate; after reaching 78K, V_g is set to 0V, and then V_{sd} is stepped to −125 V.

voltage is turned to zero, and only then is the source voltage stepped. From the measurements of the temperature dependence of the transients, it appears that charge injected into the film equilibrates fairly rapidly at room temperature. Furthermore, the measurements of gate charging, shown in Fig. 3, demonstrate that once charge is injected into the CAS, it is difficult to remove at low temperatures. Therefore, in applying a gate voltage at room temperature, the hope is to equilibrate the sample with a particular charge density at room temperature, and then to maintain that charge density after the gate voltage is turned to zero with the sample cold.

The results, for a set of transients measured with V_{sd} steps to −125 V, are shown in Figure 9. When the sample is cooled with a positive voltage on the gate, such that excess negative charge has been stored in the sample, the current transient is much smaller; conversely, cooling with a negative voltage on the gate results in a much larger current. This is consistent with the decay of the current in time; in both cases, the buildup of negative charge increases the resistance. It also suggests that at room temperature it may be possible to inject positive charge, although, given the leakage current observed even for the bare substrates (Fig. 8), it remains possible that some of the charge injected at room temperature resides in the oxide rather than within the nanocrystal film.

The parameters of the current transients depend on the size and spacing of the nanocrystals in the CAS. In

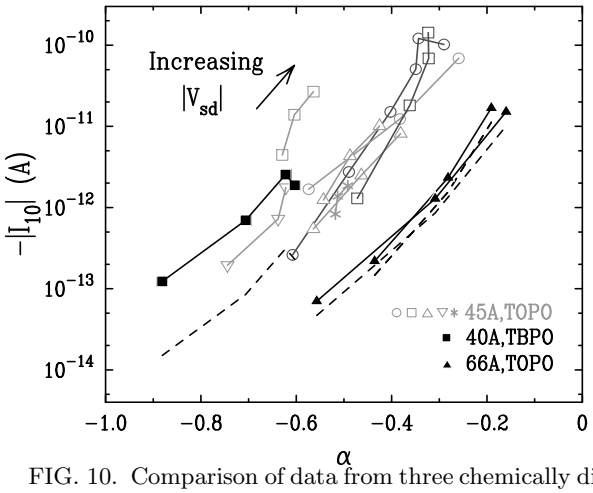

FIG. 10. Comparison of data from three chemically distinct types of samples measured on substrates with 350 nm oxides, in a plot of the amplitude of the transients at ten seconds against the exponent of the decay, obtained from power-law fits. In gray symbols are data from five different 45 Å core diameter, TOPO-capped samples, after scaling for the film thickness as described in the text. Data for the other two samples are shown before rescaling as dashed lines, and after rescaling, as filled black squares for the 40 Å core-diameter TBPO-capped sample, and filled black triangles for a 66 Å, TOPO-capped sample. The trends discussed previously, with applied voltage and temperature, are indicated with arrows.

Figure 10 we look for trends with the sample parameters by plotting the amplitude of the current transient against the decay exponent α, for a number of different samples with 1 μm length measured on substrates with 350 nm oxides. Each line connects a series of measurements on a single sample with different applied voltages (V_{sd}). The general direction of increasingly negative V_{sd} is indicated by the arrows. Data for the most commonly used type of sample, 45Å core-diameter TOPO-capped nanocrystals, are shown for five different samples. Although there is some spread among these points, data for the other two types of samples fall outside this spread. Data for a sample of 66Å core-diameter, TOPO-capped nanocrystals show somewhat smaller values for $|\alpha|$ as well as the amplitude of the transients, corresponding to a slower decay of the current. Data for a sample of 40Å core-diameter, TBPO-capped nanocrystals show larger values of $|\alpha|$, as well as smaller amplitudes.

In making comparisons between different samples, it is necessary to take the varying thicknesses of the films into account; the data in Fig. 10 correspond to films which range in thickness from 100 to 900 nm, corresponding to 20 to 180 layers of nanocrystals. As a first approximation, we have assumed that the current is proportional to the thickness of the film. The data for the standard samples in Fig. 10 has already been scaled to correct for the thickness; the clustering of these points indicates that the simple multiplicative correction is moderately successful, and suggests that the current distribution is roughly uniform for these films. There is, nonetheless, one major difference for the thinner films, shown as triangles and asterisks; although the scaled points fall in the same general area as those of the thicker samples, they span a much smaller range of α and I_{10} for the same range in V_{sd}, suggesting a change in the voltage dependence of the transients. The dependence of the current transients on film thickness requires future attention, and could be particularly interesting in the event that the two-dimensional limit could be more closely approached.

Discussion

The very high resistivity of our CAS films suggests that they contain no free carriers in the initial state. Since such free carriers are thought to quench photoluminescence[19], the high resistivity is therefore consistent with the relatively high quantum efficiencies found in similar films. However, our experiments show that at sufficiently high voltages negative charge can be injected into the CAS from gold electrodes. Furthermore, once the charge is injected, it remains in the film for very long times at temperatures below 200K. The essential questions raised by our experiments are why the charge is stored for such long times and what the relationship is between this stored charge and the observed power-law decay of the current.

We first focus on the quartz-substrate measurements, for which the gate affects neither the field nor the charge accumulation in the sample. The exponential voltage dependence of the current at fixed time might result from field emission of electrons from the Au into the CAS. In this case, one might argue that a buildup of charge near the source electrode would screen the field, reducing the the field emission. Ginger *et al.* have developed such a model to explain their observed current transients for CdSe nanocrystal arrays[8]. Using a sandwich-cell geometry, with sample thicknesses of 100-200 nm, they find a current that decays as a stretched exponential in time. In this model, charge carriers move in a transport band until they become trapped in localized states. The buildup of charge reduces the field at the contact and consequently the injection current.

We find it difficult to reconcile this model with our observations. First, it is difficult to understand why extrinsic traps should lead to current transients whose exponents change with the nanocrystal size and spacing. Second, in our measurements, orders of magnitude more charge flows to the drain than is trapped in the sample. Since the trapping probability must therefore be small, the density of trapped charge should be approximately uniform across the sample. At later times, when this uniform density of trapped charge becomes sufficient to prohibit injection from the contact, the current would not scale with the applied field. However, the current transients we observe are field-dependent at all times; there is

no evidence for a significant buildup of charge within the sample during the measurement. Furthermore, because the amplitude of the transients grows exponentially with the applied field, these measurements are fairly sensitive to deviations from field-dependence.

Alternatively, the exponential voltage dependence could arise from an exponential dependence of the hopping rate between nearest-neighbor nanocrystals. In this case, we propose that the current is not limited by injection into the sample, but rather by extraction from a space charge region which forms near the contact. This type of space-charge limited current is common in insulators with low charge density; however, for the CAS our observations differ from the conventional models of space charge limited current in two ways. First, in most systems, space-charge limited currents reach steady state when the integrated current is roughly equal to the total amount of space charge which resides in the sample. For the CAS on quartz substrates, we estimate this time to be $t < 1$ s, much shorter than the times over which we observe the power law decay. From this, we are led to propose that although the space charge region develops fairly quickly, the extraction of carriers from the space charge region decreases with time.

Second, for conventional space charge limited current, although the space charge is concentrated near the injecting contact, there is typically a long tail in the distribution which extends across the sample. As a result, in systems where space charge limited current is observed, the current generally has some dependence on the sample length as well as on the applied field[20]. However, in the CAS films we observe field-dependence of the current transients, over a time range of 1000 s for measurements on the quartz substrates. This suggests that the space charge region which limits the transport in this system is confined to a narrow region near the injecting contact. From the uncertainty associated with the scaling factor in our measurements, we estimate that this region extends no further than 100 nm from the contact, or a tenth of our smallest sample length. We note that our observations are not entirely inconsistent with those of Ginger *et al.*, whose samples were considerably shorter than those studied here; a space charge region of 100 nm in their system would extend halfway across the longest samples.

The power-law decay of the current is reminiscent of that associated with relaxation of carriers in GaAs[21]. The motion of electrons in a band of localized states with disorder has been studied in great detail[22]. This system has a Coulomb gap for single-particle excitations, and the ground state is highly degenerate. Together, these give rise to very slow relaxation times, and the system has been referred to as a Coulomb glass[23]. Such slow relaxation has been suggested as the origin of unusual phenomena in indium oxide films[24,25]. We propose that the space charge near the source electrode is a Coulomb glass. Although the space charge builds up in a very short time, the emission of electrons from the space charge region decreases with time as the Coulomb glass relaxes and the Coulomb gap grows in size. Presumably, once such a Coulomb glass relaxes it will be removed from the sample only extremely slowly after the voltage is removed; this is consistent with the sample history effects we observe as well as the charging measurements of Fig. 3. The larger exponents observed as the temperature is increased might result from more rapid relaxation of the Coulomb glass. A similar trend towards faster decay of the current is seen when changes in the array parameters lead to increased coupling between the dots, in Fig. 10. For the TBPO-capped sample, the nearest-neighbor separation is 7Å, compared to 11Å for the standard, TOPO-capped dots[10]. Because inter-dot tunneling should increase exponentially as the width of the tunnel barrier is decreased, we expect the change in capping molecules to lead to increased coupling between the dots. As for the temperature dependence, the data suggest that increased coupling between the dots leads to a faster decay of the current.

We have no quantitative theory with which to compare our results, and there are even qualitative observations that we cannot explain. For example, it is clear that the presence of a gate electrode will lead to additional space charge in the sample, so it is not surprising that the current transients are strongly modified as the gate oxide is made thinner than the spacing between source and drain. The field which extracts charge from the space charge region near the injecting contact then falls between source and gate; it increases as the gate oxide thickness decreases, and becomes less dependent on the electrode spacing. This is consistent with the data of Fig. 7, for which $I(t, V, L) = I(t, 1.6V, 2L)$ for the 1 μm and 2 μm long samples on the gated substrates, rather than the strict field dependence observed for the quartz substrates. However, we do not understand why the exponents of the current decay are larger for the gated substrates; in the Coulomb glass model the presence of more space charge should lead to slower equilibration. We also do not know how to reconcile the smaller exponents of the power-law decay of the current when we apply the voltage to the source compared with that which we observe when voltage is applied to the gate.

Our future work will focus on making samples with stronger coupling between nanocrystals. Presumbably this would make it possible to observe the hopping conductivity characteristic of the Coulomb gap.

ACKNOWLEDGMENTS

This work at MIT was supported by Award No. DMR 9808941, under the MRSEC Program of the NSF. N.Y.M. acknowledges support from an ONR Graduate Fellowship and from the Lucent Technologies Graduate Research Program for Women.

[1] C. Murray, C. Kagan, and M. Bawendi, Annual Review of Material Science **30**, 545 (2000).
[2] C. Collier, T. Vossmeyer, and J. Heath, Annual Review of Physical Chemistry **49**, 371 (1998).
[3] D. L. Klein *et al.*, Nature **389**, 699 (1997).
[4] R. Ashoori, Nature **379**, 413 (1996).
[5] M. Kastner, Physics Today **46**, 24 (1993).
[6] B. Alperson, S. Cohen, I. Rubinstein, and G. Hodes, Physical Review B **52**, R17017 (1995).
[7] D.S. Novikov, B. Kozinsky, and L.S. Levitov, cond-mat/0111345.
[8] D. Ginger and N. Greenham, Journal of Applied Physics **87**, 1361 (2000).
[9] C. Murray, D. Norris, and M. Bawendi, Journal of the American Chemical Society **115**, 8706 (1993).
[10] C. Murray, C. Kagan, and M. Bawendi, Science **270**, 1335 (1995).
[11] C. Leatherdale *et al.*, Physical Review B **62**, 2669 (2000).
[12] M. Drndic *et al.*, To be published, 2002.
[13] Other measurements, made on substrates with circular electrodes, are consistent with those shown here; for these devices, the active area of the film lies inside the outer electrode, and so the similarity of the results confirms this picture.
[14] A stretched exponential decay will always be concave downward on a log-log plot, although with $\tau, \beta \to 0$ the form approaches a straight line. Here we choose a characteristic time of $\tau = 1$ ms, an order of magnitude shorter than our earliest measurement time; longer values of τ would show still more curvature. In the data from the sandwich structures of Ref.[8], typical values of τ were 10-500 seconds.
[15] Although charge spreads into the film in all directions from the source electrode, the measured current arises only from charge which either passes into, or moves near to (relative to the thickness of the gate oxide), the drain electrode. More distant charge will be screened by the gate electrode, which is grounded for the measurement. Therefore, when estimating the possible contribution of stored charge to the measured current, we consider only the area of the film between the electrodes. Even if the entire surface of the substrate, except for the drain electrode, were charged to V_{sd}, this measurement would be sensitive only to charge around the perimeter of the electrode, leading to a correction of less than a factor of ten.
[16] In photoconductivity measurements on similar samples[11], photocurrent several orders of magnitude larger than the dark current is observed. The spectral dependence of the photocurrent is the same as the optical absorption of the nanocrystals. In the measurements discussed here, the creation of electron-hole pairs in the nanocrystals apparently makes the CAS sufficiently conducting for the charge to return to ground.
[17] W. Woo *et al.*, To be published, 2002.
[18] Here, we use the word scaling in the general sense: to say that the transients scale with the field is to say that $I(t)$ depends only on $E = V_{sd}/L$, where L is the sample length, rather than $I(t) \propto E$.
[19] D. Chepic *et al.*, Journal of Luminescence **47**, 113 (1990).
[20] K. C. Hao and W. Hwang, *Electrical transport in solids*, *International series in the science of the solid state* (Pergamon Press, 1981).
[21] D. Monroe *et al.*, Physical Review Letters **59**, 1148 (1987).
[22] A. Efros and B. Shklovskii, Journal of Physics C: Solid State Physics **8**, L49 (1975).
[23] J.H. Davies, P.A. Lee, and T.M. Rice, Physical Review B **29**, 4260 (1984).
[24] M. Ben-Chorin, Z. Ovadyahu, and M. Pollak, Physical Review B **48**, 15025 (1993).
[25] A. Vaknin, Z. Ovadyahu, and M. Pollak, Physical Review Letters **81**, 669 (1998).